The Journal of Chemical Physics

Coherent state representation of thermal correlation functions with applications to rate theory

Cite as: J. Chem. Phys. **156**, 244101 (2022); https://doi.org/10.1063/5.0088163
Submitted: 14 February 2022 • Accepted: 01 June 2022 • Accepted Manuscript Online: 02 June 2022 • Published Online: 22 June 2022

Eli Pollak, Sameernandan Upadhyayula and Jian Liu

The Journal of Chemical Physics ARTICLE scitation.org/journal/jcp

Coherent state representation of thermal correlation functions with applications to rate theory

Cite as: J. Chem. Phys. 156, 244101 (2022); doi: 10.1063/5.0088163
Submitted: 14 February 2022 • Accepted: 1 June 2022 •
Published Online: 22 June 2022

Eli Pollak,[1,a] Sameernandan Upadhyayula,[1] and Jian Liu[2,b]

AFFILIATIONS

[1] Chemical and Biological Physics Department, Weizmann Institute of Science, 76100 Rehovoth, Israel
[2] Beijing National Laboratory for Molecular Sciences, Institute of Theoretical and Computational Chemistry, College of Chemistry and Molecular Engineering, Peking University, Beijing 100871, China

[a] **Author to whom correspondence should be addressed:** eli.pollak@weizmann.ac.il.
URL: https://www.weizmann.ac.il/chembiophys/pollak/home
[b] **E-mail:** jianliupku@pku.edu.cn. **URL:** http://jianliugroup.pku.edu.cn.

ABSTRACT

A coherent state phase space representation of operators, based on the Husimi distribution, is used to derive an exact expression for the symmetrized version of thermal correlation functions. In addition to the time and temperature *independent* phase space representation of the two operators whose correlation function is of interest, the integrand includes a *non-negative* distribution function where only one imaginary time and one real time propagation are needed to compute it. The methodology is exemplified for the flux side correlation function used in rate theory. The coherent state representation necessitates the use of a smeared Gaussian flux operator whose coherent state phase space representation is identical to the classical flux expression. The resulting coherent state expression for the flux side correlation function has a number of advantages as compared to previous formulations. Since only one time propagation is needed, it is much easier to converge it with a semiclassical initial value representation. There is no need for forward–backward approximations, and in principle, the computation may be implemented on the fly. It also provides a route for analytic semiclassical approximations for the thermal rate, as exemplified by a computation of the transmission factor through symmetric and asymmetric Eckart barriers using a thawed Gaussian approximation for both imaginary and real time propagations. As a by-product, this example shows that one may obtain "good" tunneling rates using only above barrier classical trajectories even in the deep tunneling regime.

I. INTRODUCTION

Theoretical chemistry has made huge progress especially in view of the development of high speed, large memory computational facilities. The computation of molecular force fields is becoming faster and more accurate. This has led to the development of on the fly classical dynamics methods that allow for a classical simulation of molecular dynamical processes in large systems, such as energy transfer, reaction rates, and spectra.[1–3] However, even when the system is large, classical mechanics is not enough. Tunneling transitions are observable in biological systems.[4] Spectra are governed by the quantization of energy levels, be they electronic or vibrational. Despite much progress, the full quantum dynamics computation remains prohibitive due to exponential scaling of the cost with the number of degrees of freedom involved.

The challenge is to create computational methods that allow for the elucidation of quantum effects even in large systems. There are a number of important approaches used today to try and provide answers. Most notably, one uses quantum dynamics methods, such as centroid molecular dynamics (CMD),[5] ring polymer molecular dynamics (RPMD),[6] coupled coherent state dynamics,[7,8] the classical Wigner (CW) method[9] (also known as the mixed quantum classical method[10,11] or the linearized semiclassical initial value representation approach[12–16]), imaginary time

methods,[17,18] and path integral Liouville dynamics (PILD).[19,20] Semiclassical perturbation theory[21,22] has been implemented in recent years to approximate thermal rates.[23,24] Semiclassical on the fly methods have been developed to study electronic transitions,[25] internal conversion,[26] infrared spectroscopy,[27] tunneling,[28] isomerization reactions,[29] vibrationally resolved electronic spectra,[30] and more.

In this paper, we present a further alternative based on the coherent state representation of quantum operators. Assume that $\hat{H}$ is the (time-independent) Hamiltonian of the system with N degrees of freedom, which takes the standard Cartesian form

$$\hat{H} = \frac{1}{2}\hat{\mathbf{p}}^T\mathbf{M}^{-1}\hat{\mathbf{p}} + V(\hat{\mathbf{q}}), \tag{1.1}$$

where $\mathbf{M}$ is the diagonal "mass matrix" with elements $\{m_j\}$ and $\hat{\mathbf{p}}$ and $\hat{\mathbf{q}}$ are the momentum and coordinate operators, respectively. Let $\hat{A}$ and $\hat{B}$ denote operators relevant to the specific property of interest. The symmetrized form of the thermal correlation function[31] is

$$c_{AB}(t) = \frac{1}{Z_\beta}\mathrm{Tr}\left[e^{-\beta\hat{H}/2}\hat{A}e^{-\beta\hat{H}/2}\hat{K}^\dagger(t)\hat{B}\hat{K}(t)\right], \tag{1.2}$$

with $\exp(-\beta\hat{H})$ the canonical density in which $\beta = 1/(k_BT)$ is the inverse temperature, $Z_\beta = \mathrm{Tr}[\exp(-\beta\hat{H})]$ the partition function, and $\hat{K}(t) = \exp(-\frac{i}{\hbar}\hat{H}t)$ the propagator. (The relation of this symmetrized form to the standard and the Kubo-transformed form[32,33] is given through their Fourier transforms as shown in, for example, Refs. 34 and 35.)

As shown in Appendix A, the symmetrized form of the thermal correlation function [Eq. (1.2)] may, under certain circumstances, be exactly represented as

$$c_{AB}(t) = \frac{1}{Z_\beta}\int\frac{d\mathbf{p}d\mathbf{q}}{(2\pi\hbar)^N}\frac{d\mathbf{p}'d\mathbf{q}'}{(2\pi\hbar)^N}\tilde{A}_H(\mathbf{p},\mathbf{q})\tilde{B}_H(\mathbf{p}',\mathbf{q}') \times\left|\langle g(\mathbf{p},\mathbf{q};0)|e^{-\beta\hat{H}/2}\hat{K}(t)|g(\mathbf{p}',\mathbf{q}';0)\rangle\right|^2, \tag{1.3}$$

where $|g(\mathbf{p},\mathbf{q};0)\rangle$ represents the multidimensional coherent state whose coordinate representation is

$$\langle\mathbf{x}|g(\mathbf{p},\mathbf{q};t)\rangle = \left(\frac{\det(\mathbf{\Gamma}(t))}{\pi^N}\right)^{\frac{1}{4}}\exp\left(-[\mathbf{x}-\mathbf{q}(t)]^T\frac{\mathbf{\Gamma}(t)}{2} \times[\mathbf{x}-\mathbf{q}(t)] + \frac{i}{\hbar}\mathbf{p}^T(t)[\mathbf{x}-\mathbf{q}(t)]\right). \tag{1.4}$$

$\tilde{A}_H(\mathbf{p},\mathbf{q})$ and $\tilde{B}_H(\mathbf{p},\mathbf{q})$ are termed the dual functions in the Husimi phase space or equivalently the coherent state representations of the operators, $\hat{A}$ and $\hat{B}$, respectively. The definitions of the dual functions are reviewed briefly in Appendix A. For our purpose, here we note that the dual function of an operator, $\hat{O}$, in its Husimi phase space representation is given by

$$\hat{O} = \int\frac{d\mathbf{p}d\mathbf{q}}{(2\pi\hbar)^N}\tilde{O}_H(\mathbf{p},\mathbf{q})|g(\mathbf{p},\mathbf{q};0)\rangle\langle g(\mathbf{p},\mathbf{q};0)|. \tag{1.5}$$

When an operator, $\hat{A} = A(\hat{\mathbf{q}})$, is a function of only coordinate variables, the symmetrized thermal correlation function given in Eq. (1.2) may be exactly reformulated as

$$c_{AB}(t) = \frac{1}{Z_\beta}\int d\mathbf{q}\int\frac{d\mathbf{p}'d\mathbf{q}'}{(2\pi\hbar)^N}A(\mathbf{q})\tilde{B}_H(\mathbf{p}',\mathbf{q}') \times\left|\langle\mathbf{q}|e^{-\beta\hat{H}/2}\hat{K}(t)|g(\mathbf{p}',\mathbf{q}';0)\rangle\right|^2. \tag{1.6}$$

The representations given in Eqs. (1.3) and (1.6) have a number of aspects that could be beneficial when attempting to evaluate thermal correlation functions. In contrast to the original form that calls for forward and backward time propagations, the present form necessitates only one imaginary time and one real time propagation. The phase space averaging is apart from the coherent state operators, over a positive distribution as given in the term in absolute value squared. This may reduce difficulties with converging quantities that carry phases. Not less important is that, as discussed in this paper, it provides a good starting point for introducing semiclassical approximations.

The central part of this paper is presented in Sec. II, where we describe practical ways for obtaining the coherent state representations of operators. As a non-trivial example, we show how one may use the formalism to construct a new expression for the flux side correlation function that is essential for obtaining thermal reaction rates.[31] In Sec. III, we then demonstrate how the formalism may be used within the context of a thawed Gaussian semiclassical approach to estimate tunneling rates. An analytic expression for the thermal rates in one-dimensional scattering is derived and then implemented for the "classical" problem of tunneling through symmetric and asymmetric Eckart barriers. We end with a discussion of further developments and options for usage of the coherent state formalism.

II. COHERENT STATE DYNAMICS—FORMALISM

A. Coherent state representation of operators

The central concept to be used is the coherent state representation of operators, as in Eq. (1.5). In the following, we will use one-dimensional notation for the sake of simplicity, the generalization to many dimensions is straightforward. The coherent state representation of an operator $\hat{O}$ is intimately related to its Wigner representation[36] as follows:

$$O_W(p,q) = \int_{-\infty}^{\infty}d\xi\,\exp\left(\frac{i}{\hbar}p\xi\right)\left\langle q-\frac{\xi}{2}|\hat{O}|q+\frac{\xi}{2}\right\rangle. \tag{2.1}$$

Specifically, inserting the coherent state representation as in Eq. (1.5) and performing the integration over the variable ξ show that the Wigner representation of the operator is just a Gaussian transform of the coherent state representation $\tilde{O}_H(p,q)$,

$$O_W(p,q) = \int_{-\infty}^{\infty}\frac{dp'dq'}{\pi\hbar}\exp\left[-\Gamma(q-q')^2 - \frac{(p-p')^2}{\hbar^2\Gamma}\right]\tilde{O}_H(p',q'), \tag{2.2}$$

where Γ is the coherent state "width parameter." To obtain an explicit expression for the dual function $\tilde{O}_H(p,q)$, one needs the

inverse Gaussian transform.[37] As also reviewed in Appendix A, using the general phase space formulation of quantum mechanics, one finds

$$\tilde{O}_H(p,q) = \exp\left[-\frac{1}{4\Gamma}\frac{d^2}{dq^2} - \frac{\hbar^2\Gamma}{4}\frac{d^2}{dp^2}\right] O_W(p,q). \tag{2.3}$$

Using the Gaussian expansion of the inversion operator

$$\exp\left[-\frac{1}{4\Gamma}\frac{d^2}{dq^2}\right] = \sqrt{\frac{\Gamma}{\pi}}\int_{-\infty}^{\infty} dx\, \exp\left[-\Gamma x^2 + ix\frac{d}{dq}\right] \tag{2.4}$$

and noting that $\exp\left[ix\frac{d}{dq}\right]$ is just the shift operator, we find the practical formula

$$\tilde{O}_H(p,q) = \int_{-\infty}^{\infty}\frac{dp_x dx}{\pi\hbar}\exp\left[-\Gamma x^2 - \frac{1}{\hbar^2\Gamma}p_x^2\right] O_W(p+ip_x, q+ix), \tag{2.5}$$

which will serve as the basis for the derivation of coherent state representations of operators.

If operator $\hat{O}$ depends only on either the coordinate or the momenta, then as the Wigner representation will depend only on the coordinate or momentum, the same will hold true for the coherent state representation. So, for example, the dipole operator will remain unchanged from its Wigner representation. However, if one considers a density whose Wigner representation is given in terms of Dirac "delta functions," e.g., $\delta(q)$, then one finds from Eq. (2.5) that the coherent state representation is ill defined,

$$\tilde{\delta}_H(p,q) = \frac{1}{2\pi}\int_{-\infty}^{\infty} dk\, \exp\left(\frac{k^2}{4\Gamma} + ikq\right). \tag{2.6}$$

This has special implications when considering rate theory and the flux operator. The Wigner representation of the flux operator at the point $q^\ddagger$ is just the classical form $F_W(p,q;q^\ddagger) = \frac{p}{M}\delta(q-q^\ddagger)$ so that its coherent state representation would be ill defined.

The thermal rate constant (for going from left to right) is given by the flux side expression[31] as follows:

$$F_R = \lim_{t\to\infty}\mathrm{Tr}\left[\exp\left(-\frac{\beta\hat{H}}{2}\right)\hat{F}(q^\ddagger) \times \exp\left(-\frac{\beta\hat{H}}{2}\right)\hat{K}^\dagger(t)\theta(\hat{q}-q^\ddagger)\hat{K}(t)\right], \tag{2.7}$$

where $\hat{F}(q^\ddagger)$ is the flux operator defined as

$$\hat{F}(q^\ddagger) = \frac{1}{2M}\left[\hat{p}\delta(\hat{q}-q^\ddagger) + \delta(\hat{q}-q^\ddagger)\hat{p}\right], \tag{2.8}$$

and $\theta(\hat{q}-q^\ddagger)$ is the (step function) projection operator onto the region that is on the right of the barrier located at $q^\ddagger$. The flux of particles moving from left to right is, however, independent of where it is measured so that the same expression remains correct when considering the Gaussian smeared flux operator[38] (denoted by the subscript S) whose Wigner representation is readily found to be

$$F_{W,S}(p,q;q^\ddagger,\gamma) = \frac{p}{M}\sqrt{\frac{\gamma}{\pi}}\exp\left[-\gamma(q-q^\ddagger)^2\right], \tag{2.9}$$

where γ is the width parameter of the smearing function. The coherent state representation of the smeared flux operator is then found from Eq. (25) as follows:

$$\tilde{F}_{H,S}(p,q;q^\ddagger,\gamma) = \frac{p}{M}\sqrt{\frac{\Gamma\gamma}{\pi(\Gamma-\gamma)}}\exp\left[-\frac{\Gamma\gamma(q-q^\ddagger)^2}{(\Gamma-\gamma)}\right], \tag{2.10}$$

with the proviso that the width parameter Γ of the coherent state is larger than the smearing width γ. Taking the limit that $\Gamma-\gamma\to 0_+$, one finds the illuminating result:

$$\tilde{F}_{H,S}(p,q;q^\ddagger) = \frac{p}{M}\delta(q-q^\ddagger), \tag{2.11}$$

which means that using the classical expression of the flux operator for its coherent state representation is equivalent to consideration of the Gaussian smeared flux operator with a coordinate smearing function whose width is identical to that of the coherent state.

B. Coherent state flux side correlation function

As an example for the usefulness of the coherent state representation, we consider the flux side correlation function. Using the coherent state representation of the smeared flux operator, one readily integrates over the position coordinate to find that the *exact* expression for the reactive flux may be rewritten as

$$F_R = \lim_{t\to\infty}\int_0^\infty dx\int_{-\infty}^{\infty}\frac{dp}{(2\pi\hbar)} \times \frac{p}{M}\left|\left\langle x\right|\exp(-\beta\hat{H}/2)\hat{K}(t)\left|g(p,q^\ddagger)\right\rangle\right|^2. \tag{2.12}$$

This exact formulation has a classical flavor to it. It is an "average" of the velocity at the barrier location. Its numerically exact computation calls for a single time propagation rather than the usual forward–backward propagation. In addition, as shown below, it is a good starting point for semiclassical approximations. Equation (2.12) not only is of computational interest but may also be considered as a starting point for quantum transition state theories since the integrand, apart from the velocity component, is positive. The exact reactive flux is always smaller than the flux obtained with the same expression but with the momentum integration restricted to only positive momenta. For a parabolic barrier, the result of such a theory is the upper bound derived by Pechukas and McLafferty.[38]

III. THAWED GAUSSIAN RATE THEORY

The formulation of the flux side expression presented in Sec. II B is especially useful for computing semiclassical initial value approximations for the thermal rate since the propagators act directly on a coherent state. In a multidimensional system, a reasonable algorithm would be to evaluate the imaginary time thermal propagator matrix elements numerically exactly using path integral Monte Carlo methods, while the real time propagation would be implemented using, for example, the Herman–Kluk semiclassical initial value approximation.[39] This would then be a semiclassical analog of the mixed quantum classical rate theory, where one evaluates the Wigner representation of the thermal distribution

numerically exactly, while the time evolution of the projection operator is obtained from classical mechanics.[11,12] Such a semiclassical theory may be implemented on the fly and would probably be more accurate than the Wigner dynamics based mixed quantum classical theory.

The coherent state representation given in Eq. (2.12) has additional advantages, opening the door for new approximations to the thermal rate. Ever since quantum tunneling was discovered, it has been a challenge to derive an analytic expression for the thermal rate, even in one-dimensional scattering. The only analytic expression we are aware of is for the symmetric Eckart barrier. Eckart derived the exact analytic expression for the energy dependent transmission probability in 1930.[40] Yasumori and Fueki[41] using an approximation for the energy dependent probability, derived a series expansion for the rate whose terms go as $\hbar^{2n}$ and whose leading order term is identical to the exact term derived by Wigner in 1932.[42] In the following, we will demonstrate how the coherent state flux side expression of Eq. (2.12) may be used to derive an analytic expression for the thermal rate, which could be used for any simple barrier scattering problem.

For this purpose, we use a thawed Gaussian initial value representation for both the imaginary time (thermal)[43,44] and real time[45] propagators. The thawed Gaussian approximation $\hat{K}_0(\tau)$ for the imaginary time propagator $\hat{K}(\tau) = \exp(-\hat{H}\tau)$ is

$$\langle y|K_0(\tau)|x\rangle = \frac{1}{\sqrt{2\pi G(\tau)}} \exp\left(-\frac{1}{2G(\tau)}[y - x(\tau)]^2 + \gamma(\tau)\right). \quad (3.1)$$

The equations of motion are

$$\frac{dx(\tau)}{d\tau} = -G(\tau)V'(x(\tau)), \quad (3.2)$$

$$\frac{\partial G(\tau)}{\partial \tau} = -G^2(\tau)V''(x(\tau)) + \frac{\hbar^2}{M}, \quad (3.3)$$

$$\frac{d\gamma(\tau)}{d\tau} = -\frac{1}{4}G(\tau)V''(x(\tau)) - V(x(\tau)), \quad (3.4)$$

with initial conditions

$$x(\tau \approx 0) = x, \qquad G(\tau \approx 0) = \frac{\hbar^2}{M}\tau, \qquad \gamma(\tau \approx 0) = -\tau V(x). \quad (3.5)$$

The thawed Gaussian approximation in real time is

$$\langle x|\exp\left(-\frac{iHt}{\hbar}\right)|g(p,q)\rangle = \left(\frac{Re\Gamma_t}{\pi}\right)^{1/4} \exp\left[-\frac{\Gamma_t}{2}(x - q_t)^2 + \frac{i}{\hbar}p_t(x - q_t) + \frac{i}{\hbar}W(p_t, q_t)\right]. \quad (3.6)$$

The associated real time equations of motion are Hamilton's equations of motion for the time dependent momentum and coordinate (denoted as p_t and q_t, respectively) and a complex equation for the time evolving width parameter,

$$\dot{q}_t = \frac{p_t}{M}, \quad (3.7)$$

$$\dot{p}_t = -V'(q_t), \quad (3.8)$$

$$i\hbar\dot{\Gamma}_t = -V''(q_t) + \frac{\hbar^2\Gamma_t^2}{M}. \quad (3.9)$$

The action is

$$W(p_t, q_t) = \int_0^t dt'\left[\frac{p_{t'}^2}{2M} - V(q_{t'})\right] - \frac{\hbar^2}{2M}\int_0^t dt' Re\Gamma_{t'}, \quad (3.10)$$

but it is irrelevant for our purposes as it disappears when considering the absolute value squared of the matrix element appearing in Eq. (2.12). This is a central advantage of the present formulation.

With these preliminaries, it becomes possible to derive an analytic expression for the thermal rate of crossing a simple barrier potential $V(q)$ whose generic structure is shown schematically in Fig. 1. At reactants ($q \to -\infty$), the potential is constant with magnitude 0. In the product region ($q \to +\infty$), the potential is again constant with energy $-\Delta V$ such that ΔV is the exoergicity of the reaction. The barrier, with barrier height $V^{\ddagger}$ relative to reactants, is located somewhere in between at $q^{\ddagger}$. The classical Hamiltonian governing the equations of motion for the phase space variables is assumed to be of the form

$$H_{cl} = \frac{p^2}{2M} + V(q). \quad (3.11)$$

In the classical limit (or equivalently the high temperature limit of the quantum rate), the thermal flux is given by

$$F_{cl} = \lim_{\hbar\to 0} F_R = \frac{1}{2\pi\hbar\beta}\exp\left(-\beta V^{\ddagger}\right). \quad (3.12)$$

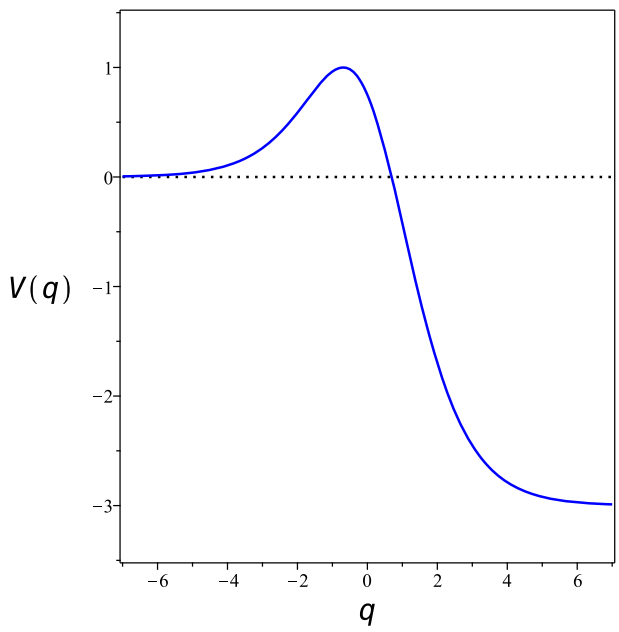

FIG. 1. Schematic representation of the barrier potentials considered. In this specific case, the barrier height is (in arbitrary units) $V^{\ddagger} = 1$, and the exoergicity is $\Delta V = 3$.

This allows us to define the transmission factor as the ratio of the semiclassical thawed Gaussian reactive flux to the classical reactive flux. The resulting expression whose derivation is presented in Appendix B is

$$P_R = \frac{1}{2}\sqrt{\left(\frac{\hbar^2\Gamma\beta}{2M}+1\right)}\exp\left(\frac{\hbar^2\Gamma\beta^2\left(V^\ddagger+\Delta V\right)}{\left(\hbar^2\Gamma\beta+2M\right)}\right)\times\left[\mathrm{erf}\left(\sqrt{\frac{2M^2\left(V^\ddagger+\Delta V\right)}{\hbar^2\Gamma\left(\hbar^2\Gamma\frac{\beta}{2}+M\right)}}\right)+1\right]+\frac{1}{2}\sqrt{\left(\frac{\hbar^2\Gamma\beta}{2M}+1\right)}\exp\left(\frac{\hbar^2\Gamma\beta^2V^\ddagger}{\hbar^2\Gamma\beta+2M}\right)\times\left[\mathrm{erf}\left(\sqrt{\frac{2M^2V^\ddagger}{\hbar^2\Gamma\left(\hbar^2\Gamma\frac{\beta}{2}+M\right)}}\right)-1\right]+\frac{\exp\left(\beta V^\ddagger\right)}{2}\times\left[1-\mathrm{erf}\left(\sqrt{\frac{2MV^\ddagger}{\hbar^2\Gamma}}\right)\right]+\frac{1}{2}\exp\left[\beta\left(V^\ddagger+\Delta V\right)\right]\times\left[1-\mathrm{erf}\left(\sqrt{\frac{2M\left(V^\ddagger+\Delta V\right)}{\hbar^2\Gamma}}\right)\right]. \tag{3.13}$$

For a symmetric barrier, this reduces to the simpler expression

$$P_{R,sym} = \sqrt{\frac{\left(\hbar^2\Gamma\frac{\beta}{2}+M\right)}{M}}\exp\left[\frac{\hbar^2\Gamma\beta^2V^\ddagger}{\left(\hbar^2\Gamma\beta+2M\right)}\right]\times\mathrm{erf}\left(\sqrt{\frac{2M^2V^\ddagger}{\hbar^2\Gamma\left(\hbar^2\Gamma\frac{\beta}{2}+M\right)}}\right)+\exp\left(\beta V^\ddagger\right)\left[1-\mathrm{erf}\left(\sqrt{\frac{2MV^\ddagger}{\hbar^2\Gamma}}\right)\right]. \tag{3.14}$$

The thawed Gaussian propagators in real and imaginary time are exact for a parabolic barrier so that using them in Eq. (2.12) leads to the exact quantum transmission probability for the parabolic barrier. The present expressions are different. In deriving Eqs. (3.13) and (3.14), we made use of the asymptotic constant structure of the potential, which is not the case for the parabolic barrier, and therefore, they are not applicable directly to the parabolic barrier case, although, as we shall see below, they do give the correct high temperature quantum corrections.

The analytic expressions derived for the one-dimensional transmission factor are not yet complete, since they depend on the width parameter Γ used for the smeared flux operator or equivalently for the coherent states. This may be considered a disadvantage, but we will argue that it is an important advantage, as it provides further flexibility. Our strategy for choosing the width parameter will be to assure that the analytical expression becomes exact in the small $\hbar$ limit, where one may obtain an expansion of the exact rate constant in powers of $\hbar^2$.

For example, Wigner derived in 1932 the exact leading order correction term to the rate[42] for a symmetric barrier, with barrier frequency ω,

$$P = 1+\frac{\hbar^2\beta^2\omega^2}{24}\left(1+\frac{1}{4M^2\beta\omega^4}\frac{\partial^4V(q)}{\partial q^4}|_{q=0}\right)+O\left(\hbar^4\right). \tag{3.15}$$

On the other hand, expanding the thawed Gaussian expression for the transmission factor [Eq. (3.13)] gives

$$P_R = 1+\frac{\hbar^2\Gamma\beta}{2M}\left(\frac{1}{2}+\beta\left(V^\ddagger+\Delta V\right)\right)+\frac{\hbar^4\Gamma^2\beta^2}{8M^2}\times\left[\left(\beta\left(V^\ddagger+\Delta V\right)\right)^2-\left(\beta\left(V^\ddagger+\Delta V\right)\right)-\frac{1}{4}\right]+O\left(\hbar^6\right). \tag{3.16}$$

We may then expand the width parameter in terms of $\hbar$ as

$$\Gamma = \Gamma_0+\hbar^2\Gamma_1 \tag{3.17}$$

and derive the relevant expressions for the coefficients Γ_0 and Γ_1 by comparing with the exact expansion of the rate up to $\hbar^4$. These may then be extrapolated to low temperature as demonstrated below for the benchmark Eckart barriers, for which other approximate methods have been tested.[11,18,46–50]

A. Symmetric Eckart barrier

The symmetric Eckart barrier potential Hamiltonian is

$$H = \frac{p_x^2}{2M}+\frac{V^\ddagger}{\cosh^2\left(\frac{x}{d}\right)}, \tag{3.18}$$

and due to the symmetry, the expression for the reaction probability simplifies considerably as in Eq. (3.14). For the symmetric Eckart barrier, the barrier frequency is related to the barrier height as

$$\omega^2 = \frac{2V^\ddagger}{Md^2}. \tag{3.19}$$

In these reduced variables, the transmission factor expression [Eq. (3.14)] becomes a function of the following three reduced variables:

$$\tilde{\Gamma} = d^2\Gamma,\quad \alpha = \frac{\hbar}{Md^2\,\omega},\quad \tilde{\tau} = \frac{\hbar\omega\beta}{2}, \tag{3.20}$$

and we note that the reduced barrier height is

$$\beta V^\ddagger = \frac{\tilde{\tau}}{\alpha}. \tag{3.21}$$

The transmission factor is then

$$P_R = \exp\left(\frac{\tilde{\tau}}{\alpha}\right)\left[\sqrt{1+\tilde{\tau}\tilde{\Gamma}\alpha}\,\exp\left(-\frac{\tilde{\tau}}{\alpha\left(\alpha\tilde{\tau}\tilde{\Gamma}+1\right)}\right)\times\mathrm{erf}\left(\sqrt{\frac{1}{\tilde{\Gamma}\alpha^2\left(\alpha\tilde{\tau}\tilde{\Gamma}+1\right)}}\right)+\left[1-\mathrm{erf}\left(\sqrt{\frac{1}{\tilde{\Gamma}\alpha^2}}\right)\right]\right]. \tag{3.22}$$

As shown in Appendix C, the leading order expansion in terms of $\hbar^2$ and $\hbar^4$ (or equivalently α^2 and α^4) of the exact rate for the symmetric Eckart barrier is

$$P(\beta) = 1 + \frac{\alpha^2\beta V^\ddagger}{6}\left(1+\beta V^\ddagger\right) + \frac{\alpha^4\left(\beta V^\ddagger\right)^2}{360} \times \left[9 + 7\left(\beta V^\ddagger\right)^2 - 6\beta V^\ddagger\right] + O\left(\alpha^6\right). \tag{3.23}$$

Using the expansion of the width parameter in terms of $\hbar^2$ as in Eq. (3.17), one readily finds

$$d^2\Gamma_0 = \frac{\left(1+\beta V^\ddagger\right)}{3\left(1+2\beta V^\ddagger\right)}, \tag{3.24}$$

$$d^2\hbar^2\Gamma_1 = \frac{\alpha^2\beta V^\ddagger}{90\left(1+2\beta V^\ddagger\right)^3}\left[4\left(\beta V^\ddagger\right)^4 + 2\left(\beta V^\ddagger\right)^3 + 22\left(\beta V^\ddagger\right)^2 + 30\left(\beta V^\ddagger\right) + 7\right]. \tag{3.25}$$

These results are instructive. For a fixed value of α, one notes that in the high temperature limit, that is, in the limit that $\beta V^\ddagger \to 0$, the width parameter goes to a constant value of $\frac{1}{3}$, while in the low temperature limit, that is, when $\beta V^\ddagger \to \infty$, the width parameter increases to $\frac{\alpha^2}{180}\left(\beta V^\ddagger\right)^2$. Classical barrier crossing occurs only when the momentum at the barrier is positive. A large spatial width parameter implies a narrow smeared flux function in coordinate space, which implies a broad function in momentum space. Increasing the momentum width of the initial distribution implies a higher probability for the above barrier momenta and thus barrier crossing. In this thawed Gaussian picture, tunneling occurs solely by those trajectories initiated in the reactant region whose momentum is associated with an energy that is greater than the barrier height. The probability for attaining this momentum depends on the coherent state. The narrower it is in the coordinate space, the larger its momentum width, and thus, the probability for higher momentum increases. As the temperature is lowered, the increase in the spatial width parameter increases the probability of higher momenta, thus increasing the transmission probability. In the thawed Gaussian theory, tunneling is attained purely by the above barrier classical trajectories even in the deep tunneling regime. This gives a rather different picture from that considered elsewhere according to which deep tunneling cannot be ascribed to the above barrier classical trajectories[51] or that it is affected by Gaussian weighted jumps between classical paths.[52]

We apply this theory to the well-studied example for the symmetric Eckart barrier that corresponds to a model of the hydrogen exchange reaction with $\alpha = \pi/12$. In the right most column of Table I, we show the transmission probabilities obtained using the expansion of the rate to fourth order as in Eq. (3.23). As may be inferred from this table, using this high temperature limit, one obtains accurate results only up to $\hbar\beta\omega^\ddagger = 4$. For lower temperatures, perhaps not unexpectedly, using the first two terms in the high temperature expansion does not account well for the tunneling transmission factors at lower energy. The numerically exact transmission factors are shown in the second column from the left. The third column from the right shows the results obtained from the thawed Gaussian expression for the transmission factor [Eq. (3.22)] using only the leading order term for the width parameter (Γ_0) as in Eq. (3.24). Although in this case we used only the lowest order term of order $\hbar^2$, the result is as good as the high temperature limit, also giving quite accurate rates, provided that $\hbar\beta\omega \le 4$. It is instructive to compare these results with the parabolic barrier approximation

$$P_{pb} = \frac{\tau}{\sin(\tau)} \tag{3.26}$$

whose values are shown in the second column from the right. One notes that systematically, in the high temperature region, the parabolic barrier expression *under*estimates the exact transmission probability.

This is not a trivial observation. As already noted by Wigner,[42] the classical Wigner approximation as we call it today does not include the fourth derivative term and therefore is too small. This presents a challenge also to other thermal rate theories, such as

TABLE I. Transmission factors for the symmetric barrier case. The various columns are obtained for different estimates of the rate, as explained in the text.

$\hbar\beta\omega$	Exact	$\tilde{\Gamma}_0\left[1+\ln\left(1+\frac{\tilde{\Gamma}_1}{\tilde{\Gamma}_0}\right)\right]$	$\left(\tilde{\Gamma}_0+\tilde{\Gamma}_1\right)$	$\tilde{\Gamma}_0$	P_{pb}	High T limit
1.5	1.130	1.133	1.133	1.130	1.100	1.132
2	1.224	1.230	1.230	1.223	1.188	1.227
3	1.525	1.548	1.549	1.511	1.504	1.528
4	2.071	2.143	2.151	1.998	2.200	2.037
6	5.199	5.673	5.890	4.217	21.26	4.104
8	21.77	24.25	28.62	11.18	⋯	8.567
10	161.9	168.9	271.6	36.33	⋯	17.04
12	1973.3	1842	5154	141.7	⋯	31.58
14	34 057	29 398	184 523	651.3	⋯	54.75
16	7.404×10^5	6.376×10^5	1.105×10^7	3472	⋯	89.54
18	1.882×10^7	1.756×10^7	9.591×10^8	21 190	⋯	139.4
20	5.344×10^8	5.795×10^8	10.50×10^{10}	147 438		208.4

Miller's semiclassical theory,[21,22] centroid,[48] or ring polymer molecular dynamics,[49,50] which typically reduce to the parabolic barrier limit but do not obtain the added term as derived by Wigner.

As may be seen from the results presented in Table I, using only $\tilde{\Gamma}_0$, we obtain an estimate that is too low as the temperature is reduced. Inspection of Eq. (3.24) shows that $d^2\Gamma_0$ is an increasing function of the temperature, varying from the value of 1/3 at high temperature to 1/6 at low temperature. For this reason, it cannot account for the deep tunneling region. The second term increases significantly when the temperature is lowered. Therefore, adding the term with $\tilde{\Gamma}_1$ gives somewhat better results as shown in the middle column of this table. However, empirically, we notice that the value of $\tilde{\Gamma}$ rises too rapidly as the temperature is lowered and the resulting transmission factors are too high. Inspection of Eq. (3.25) shows that Γ_1 diverges as $(\beta V^\ddagger)^2$ when $\beta \to \infty$. On the other hand, we know, in general, that in the limit of $\beta \to \infty$, the true transmission factor should go to zero due to quantum reflection, and the semiclassical instanton result will go to a finite value. It is thus clear that to obtain good agreement with the numerically exact results at low temperature, one should mitigate the rapid rise of Γ_1 with β. With this in mind, we used an ansatz that recovers the high temperature estimate of $\tilde{\Gamma}_0 + \tilde{\Gamma}_1$ but prevents the width parameter from rising too quickly as β becomes large,

$$\tilde{\Gamma} = \tilde{\Gamma}_0\left[1 + \ln\left(1 + \frac{\tilde{\Gamma}_1}{\tilde{\Gamma}_0}\right)\right]. \tag{3.27}$$

This ansatz does not call for any additional information but provides a more reasonable extrapolation of the width parameter as one goes to low temperature. As may be seen from the third column from the left of Table I, this ansatz gives quite accurate results for the transmission factor, covering over eight orders of magnitude in the transmission factor, comparable in quality to those obtained in Ref. 18. For the symmetric Eckart barrier, the thawed Gaussian coherent state flux side expression leads to an accurate analytic estimate of the thermal rate.

B. Asymmetric Eckart barrier

The asymmetric Eckart barrier potential has the form

$$V(x) = \frac{V_1 - V_2}{1 + \exp\left(-\frac{x}{d}\right)} + \frac{\left(\sqrt{V_1} + \sqrt{V_2}\right)^2}{4\cosh^2\left(\frac{x}{2d}\right)} \tag{3.28}$$

such that the barrier is located at

$$x^\ddagger = d\,\ln\left(\frac{\left(\sqrt{V_1} + \sqrt{V_2}\right)^2 - (V_2 - V_1)}{\left(\sqrt{V_1} + \sqrt{V_2}\right)^2 + (V_2 - V_1)}\right), \tag{3.29}$$

and the barrier height is

$$V^\ddagger = V_1. \tag{3.30}$$

The exoergicity is

$$\Delta V = V_2 - V_1. \tag{3.31}$$

TABLE II. Transmission factors for the asymmetric barrier case. The notation is as in Table I except that the parabolic barrier estimate is not included.

$\hbar\beta\omega$	Exact	$\tilde{\Gamma}_0\left[1 + \ln\left(1 + \frac{\tilde{\Gamma}_1}{\tilde{\Gamma}_0}\right)\right]$	$\tilde{\Gamma}_0 + \tilde{\Gamma}_1$	$\tilde{\Gamma}_0$	High T limit
1.5	1.109	1.109	1.111	1.11	1.109
2	1.195	1.195	1.195	1.198	1.195
3	1.480	1.479	1.479	1.481	1.471
4	2.015	2.013	2.014	1.982	1.945
6	5.322	5.274	5.325	4.477	3.883
8	26.10	24.83	26.81	13.68	8.08
10	251.6	241.9	333	56.1	16.1
12	4068	5413	13 653	305	29.8
14	0.9055×10^5	2.946×10^5	2.469×10^6	2185	51.7

The parameters we use are the same as employed in Ref. 11 such that $V_2 = 4V_1$ and $\Delta V = 3V^\ddagger$. For this specific case, the barrier frequency is related to the barrier height by

$$\omega^2 = \frac{8V^\ddagger}{9Md^2}. \tag{3.32}$$

Other parameters are scaled as for the symmetric case [see Eq. (3.20)]. The parameter α was chosen such that the barrier height is identical to the barrier height of the symmetric Eckart barrier, that is, $\alpha = \frac{3\pi}{16}$.

For the asymmetric case, there is no known analytic expansion of the rate as a function of $\hbar^2$. We therefore resorted to a numerical strategy to determine the temperature dependence of the width parameter, as described in more detail in Appendix D. Briefly, we computed numerically the exact rate constant in the range $0 \le \hbar\beta\omega \le 0.8$ and fit it to a fourth order polynomial in the variable $\tau = \frac{\hbar\beta\omega}{2}$. This was then used to determine the width parameters $\tilde{\Gamma}_0$ and $\tilde{\Gamma}_1$. The results are given in Table II. As in the symmetric case, using the width parameter $\tilde{\Gamma}_0$ does not account for the significant tunneling at low temperatures. Using $\tilde{\Gamma}_0 + \tilde{\Gamma}_1$ gives reasonable results for $\hbar\beta\omega \le 8$, and using the ansatz of Eq. (3.27) gives accurate results for $\hbar\beta\omega \le 12$. The results obtained by the analytic expression are more accurate than those obtained by a variety of different approximate methods to determine the rate constant.

IV. DISCUSSION

The highlights of this paper are as follows:

- a general formalism for the computation of thermal correlation functions based on the coherent state representation of operators,
- a general formula for the computation of the coherent state representation of the operators,
- a coherent state based formulation of the flux side correlation function using a smeared flux operator,
- derivation of the coherent state representation of the flux operator as its classical representation,
- application of the coherent state flux side correlation function to derive an analytic formula for the thermal tunneling rate through simple barriers based on thawed Gaussian propagators, and

- application of the resulting theory to the symmetric and asymmetric Eckart barrier tunneling rates.

The implications of these results are numerous. The general expression of the correlation function using coherent states has a number of advantages:

- The resulting expression presents an average of a positive temperature and time dependent distribution function, which should be helpful in applying the formalism using numerically exact methods. The numerical difficulty caused by the highly oscillatory structure of the integrand is much alleviated, and this should facilitate the convergence of Monte Carlo methods.
- In contrast to the "standard" methods that imply a forward and backward time propagation, the coherent state form presented in Eq. (1.5) involves only a single forward time propagation. This reduces the numerical effort when using semiclassical initial value representations of the propagator.
- The use of coherent states has the advantage that it is directly amenable to semiclassical initial value propagation, as also exemplified for the flux side correlation function combined with thawed Gaussian propagation.

As discussed in this paper, a necessary condition for the application of the coherent state correlation function representation is the construction of a practical method for the computation of the coherent state representation of operators. For this purpose, we derived an explicit inversion formula connecting between the Wigner representation of an operator and its coherent state representation. This formula highlights also the difficulties especially when dealing with the Dirac delta function or step function operators. For the flux side correlation function, this impediment was removed through the use of a Gaussian smeared flux operator.[38] The resulting coherent state representation of the flux operator is just the classical form.

The versatility of the new expression for the flux side correlation function is especially useful in the context of thawed Gaussian approximations to the wavefunction. Using the thawed Gaussian semiclassical approximation for both the thermal and real time propagators, we derived an analytic expression for the thermal rate. The result depends, however, on the choice of the width parameter used to smear the flux operator. This may be considered a weakness, but conversely, it may be considered an added strength of the theory. We showed that by judicious choice of the temperature dependence of the width parameter, one could obtain very reasonable approximations to the transmission factor for both the symmetric and asymmetric cases. Specifically, in view of machine learning algorithms, one may perhaps utilize this freedom of choice for the width parameter to learn what would be the most general optimal function to use. For the Eckart barrier, one knows the exact transmission factor at each temperature. One can then use this knowledge to fit the width parameter so that the thawed Gaussian theory would give the exact transmission factor. Such an inversion is shown in Fig. 2 for the symmetric case (left) used in Table I and the asymmetric case (right) considered in Table II.

These plots are noteworthy for a number of reasons. The coherent state reactive flux expression given in Eq. (2.12) is exact and so does not depend on the choice of the width parameter Γ. This means that, in principle, the width parameter should not vary with the temperature. Inspection of Fig. 2 shows that for both the symmetric and asymmetric barrier cases, the width parameter hardly changes

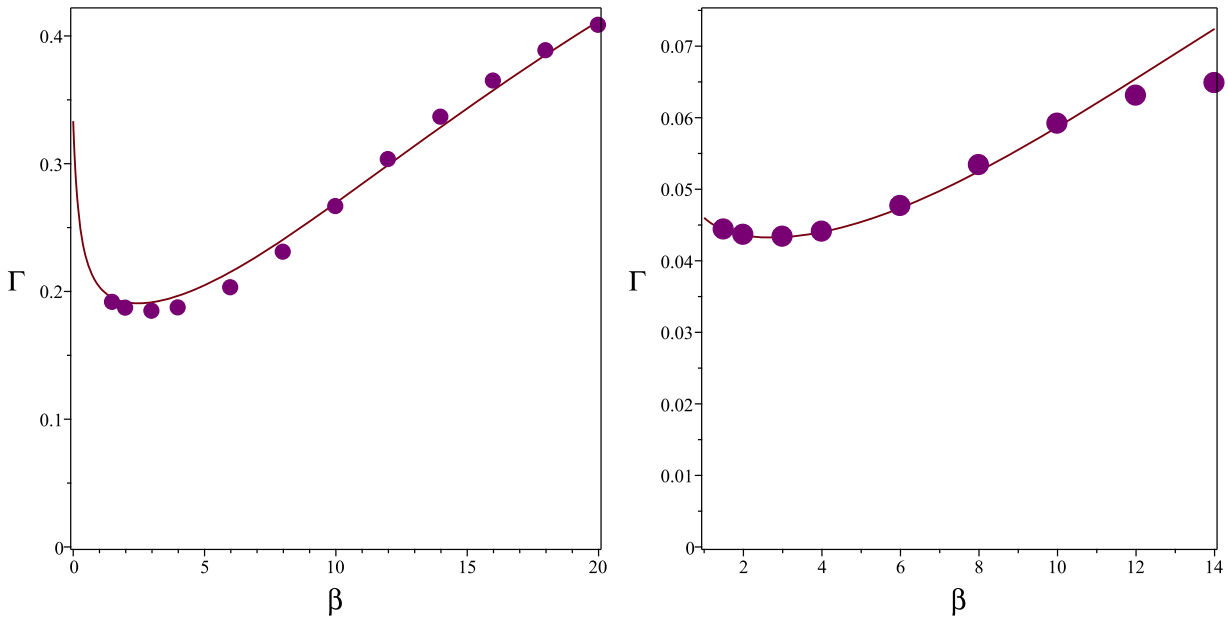

FIG. 2. Temperature dependence of the width parameter. The x-axis shows the reduced temperature $\hbar\beta\omega$. The solid circles show the value of the (reduced) width parameter that would give the exact rate; the solid line is the value obtained from Eq. (3.27). The left panel is for the symmetric case (see Table I), and the right panel is for the asymmetric case (see Table II).

for temperatures above the crossover temperature ($\beta = 2\pi$), indicating the validity of the thawed Gaussian estimate in this temperature range. Moreover, over all the temperature range considered, the "exact" width parameter changes by a factor of 2 in the symmetric case and only 50% in the asymmetric case. We will investigate in future work whether a more accurate estimate of the imaginary time propagator would lead to a theory, whereby this dependence is further reduced, leading to a more accurate theory.

This figure also demonstrates that the optimal value of the width parameter changes in a smooth way as a function of temperature and generally increases as the temperature is lowered. There is some real physics underlying this structure. Increasing the width parameter implies that the width of the momentum distribution associated with the coherent states increases, giving a higher probability for momenta whose energy supersedes the barrier energy. The fact that for any temperature there exists a value of the width parameter that gives the exact transmission factor implies that even deep tunneling may be represented correctly in terms of the above barrier trajectories only.

Why do we stress this? The present application was limited to one-dimensional scattering. However, there is nothing in the formalism that limits its use to one dimension. In multidimensional applications, there is a coherent state phase space associated with each degree of freedom. Each one of these has a separate width parameter. For many degrees of freedom, the most general coherent state would have a symmetric matrix of width parameters, all of which could be optimized through the use of a machine learning algorithm.[53] The thawed Gaussian theories have been considered extensively in recent years in the context of complex systems, and so, these are also known in the multidimensional case.[54,55]

The comparison between the "exact" width parameters and those used in the approximate determination of the width parameters through the high temperature expansion is also instructive. The expansion used not only is quantitative for a large range of temperatures for a given potential but also correctly describes the order of magnitude difference between the magnitude of the width parameter in the symmetric and asymmetric cases considered.

These results should create renewed interest in the computation of thermal correlation functions at high temperature even though the actual quantum effect is rather limited. We note that most approximate methods employed for thermal rates do not get the correct high temperature limit. They reduce to the parabolic barrier limit, but as already stressed by Wigner, this is not the whole story.

In principle, the exact evaluation of the coherent state representation of the flux side correlation function [Eq. (1.6)] gives a reaction rate that is independent of the choice of the dividing surface. This independence is, however, not satisfied by the thawed Gaussian approach used in this paper. To improve upon the present results, one may consider varying the location of the dividing surface[10] and use that location at which the derivative of the approximate flux with respect to the location of the dividing surface vanishes. In the symmetric case, this will almost always be the barrier top; however, this is not the case in the asymmetric case, where such optimization will usually improve the estimate.[11,15]

Perhaps not less important is the fact that the thawed Gaussian is just a zeroth order term in a time dependent perturbation theory expansion of the exact propagator[35,57–59] so that one may improve systematically upon the zeroth order thawed Gaussian theory used here. The added expense in computing the first order term is no greater than the expense needed to compute the zeroth order term with the Herman–Kluk initial value semiclassical representation of the propagator.[39] Moreover, one may use this first order correction term as a different strategy for choosing the width parameter, namely, by choosing the value of the width parameter that minimizes the relative magnitude of the first order term.

To summarize, the coherent state approach to thermal correlation functions seems promising. Some of its practical advantages have been demonstrated here for thermal reaction rate estimates and especially for one-dimensional Eckart barriers, but much is left to be done to demonstrate its utility also in the context of other desirable thermal correlation functions for larger molecular systems.

ACKNOWLEDGMENTS

We thank Professor J. Cao, Professor R. Martinazzo, and Professor J. Shao for numerous discussions. This work was graciously supported by a joint grant of the Natural National Science Foundation of China (NSFC) under Grant No. 21961142017 and the Israel Science Foundation (ISF) under Grant No. 2965/19.

AUTHOR DECLARATIONS

Conflict of Interest

The authors have no conflicts to disclose.

Author Contributions

Eli Pollak: Conceptualization (equal); Formal analysis (lead); Funding acquisition (equal); Investigation (lead); Methodology (equal); Writing – original draft (lead); Writing – review & editing (equal). **Sameernandan Upadhyayula:** Investigation (supporting). **Jian Liu:** Conceptualization (equal); Resources (equal).

DATA AVAILABILITY

The data that support the findings of this study are available from the corresponding author upon reasonable request.

APPENDIX A: PHASE SPACE REPRESENTATION OF A QUANTUM OPERATOR

The phase space formulation of quantum mechanics with coordinate-momentum variables[60–64] is formulated such that the trace of a product of two quantum operators is equivalent to an integral of two phase space functions, i.e.,

$$\mathrm{Tr}\left[\hat{A}\hat{B}\right] = \frac{1}{(2\pi\hbar)^N}\int d\mathbf{q}d\mathbf{p}A_C(\mathbf{x},\mathbf{p})\tilde{B}_C(\mathbf{q},\mathbf{p}), \tag{A1}$$

where

$$A_C(\mathbf{q},\mathbf{p}) = \mathrm{Tr}\left[\hat{A}\hat{K}(\mathbf{q},\mathbf{p})\right] \tag{A2}$$

and

$$\tilde{B}_C(\mathbf{q},\mathbf{p}) = \mathrm{Tr}\left[\hat{K}^{-1}(\mathbf{q},\mathbf{p})\hat{B}\right]. \tag{A3}$$

Conversely,

$$\hat{A} = \frac{1}{(2\pi\hbar)^N}\int d\mathbf{q}d\mathbf{p}A_C(\mathbf{q},\mathbf{p})\hat{K}^{-1}(\mathbf{q},\mathbf{p}),$$
$$\hat{B} = \frac{1}{(2\pi\hbar)^N}\int d\mathbf{q}d\mathbf{p}\tilde{B}_C(\mathbf{q},\mathbf{p})\hat{K}(\mathbf{q},\mathbf{p}). \quad \text{(A4)}$$

In Eqs. (A1)–(A4), the mapping kernel $\hat{K}(\mathbf{q},\mathbf{p})$ and the corresponding inverse satisfy the normalization,

$$\mathrm{Tr}\left[\hat{K}(\mathbf{q},\mathbf{p})\right] = \mathrm{Tr}\left[\hat{K}^{-1}(\mathbf{q},\mathbf{p})\right] = 1 \quad \text{(A5)}$$

and

$$\frac{1}{(2\pi\hbar)^N}\int d\mathbf{q}d\mathbf{p}\hat{K}(\mathbf{q},\mathbf{p}) = \frac{1}{(2\pi\hbar)^N}\int d\mathbf{q}d\mathbf{p}\hat{K}^{-1}(\mathbf{q},\mathbf{p}) = \hat{I}. \quad \text{(A6)}$$

Here, $\hat{I}$ is the identity operator.

Since we are considering in this paper a continuous-variable quantum system, the mapping phase space involved is *infinite*. The integral measure is chosen to be $(2\pi\hbar)^{-N}d\mathbf{q}d\mathbf{p}$. Recent progress implies that *constraint* coordinate-momentum phase space is employed for the discrete-variable quantum system.[63,65–67] Liu and co-workers have suggested that it is more comprehensive to employ the kernel $\hat{K}(\mathbf{q},\mathbf{p})$ and its inverse for mapping the coordinate-momentum phase space for a composite system that includes both continuous and discrete variables.[63,65–67] Even when the continuous-variable system is studied, it is also more convenient to reformulate Cohen's scheme[60,62] in this way[35] so that one readily obtains the phase space representation of a quantum operator from Eq. (A4) and the transformation between two different phase space representations.

The mapping kernel for describing the continuous-variable system is

$$\hat{K}(\mathbf{q},\mathbf{p}) = \left(\frac{\hbar}{2\pi}\right)^N\int d\boldsymbol{\zeta}d\boldsymbol{\eta}e^{i\boldsymbol{\zeta}^T(\hat{\mathbf{q}}-\mathbf{q})+i\boldsymbol{\eta}^T(\hat{\mathbf{p}}-\mathbf{p})}f(\boldsymbol{\zeta},\boldsymbol{\eta}), \quad \text{(A7)}$$

and the corresponding inverse kernel is

$$\hat{K}^{-1}(\mathbf{q},\mathbf{p}) = \left(\frac{\hbar}{2\pi}\right)^N\int d\boldsymbol{\zeta}d\boldsymbol{\eta}e^{-i\boldsymbol{\zeta}^T(\hat{\mathbf{q}}-\mathbf{q})-i\boldsymbol{\eta}^T(\hat{\mathbf{p}}-\mathbf{p})}\frac{1}{f(\boldsymbol{\zeta},\boldsymbol{\eta})}, \quad \text{(A8)}$$

where $f(\boldsymbol{\zeta},\boldsymbol{\eta})$ is a scalar function that defines the corresponding phase space. For example, the choice

$$f(\boldsymbol{\zeta},\boldsymbol{\eta}) = 1 \quad \text{(A9)}$$

gives the Wigner function,[68] and the choice

$$f(\boldsymbol{\zeta},\boldsymbol{\eta}) = \exp\left(-\frac{\boldsymbol{\zeta}^T\boldsymbol{\Gamma}^{-1}\boldsymbol{\zeta}}{4} - \frac{\hbar^2}{4}\boldsymbol{\eta}^T\boldsymbol{\Gamma}\boldsymbol{\eta}\right) \quad \text{(A10)}$$

yields the Husimi function.[69]

When the Wigner function is used, the kernel is identical to its corresponding inverse. Equations (A2) and (A3) take the same form, i.e.,

$$B_W(\mathbf{p},\mathbf{q}) = \tilde{B}_W(\mathbf{p},\mathbf{q}) = \left(\frac{\hbar}{2\pi}\right)^N\int d\boldsymbol{\zeta}d\boldsymbol{\eta}\,\mathrm{Tr}\left[e^{i\boldsymbol{\zeta}^T(\hat{\mathbf{q}}-\mathbf{q})+i\boldsymbol{\eta}^T(\hat{\mathbf{p}}-\mathbf{p})}\hat{B}\right] = \int d\mathbf{y}e^{i\mathbf{y}^T\mathbf{p}/\hbar}\left\langle\mathbf{q}-\frac{\mathbf{y}}{2}\middle|\hat{B}\middle|\mathbf{q}+\frac{\mathbf{y}}{2}\right\rangle. \quad \text{(A11)}$$

Equation (A4) produces the Wigner phase space representation of operator $\hat{B}$, i.e.,

$$\hat{B} = \frac{1}{(2\pi\hbar)^N}\int d\mathbf{q}d\mathbf{p}d\mathbf{y}\tilde{B}_W(\mathbf{q},\mathbf{p})e^{i\mathbf{y}^T\mathbf{p}/\hbar}\left|\mathbf{q}+\frac{\mathbf{y}}{2}\right\rangle\left\langle\mathbf{q}-\frac{\mathbf{y}}{2}\right|. \quad \text{(A12)}$$

When the operator $\hat{B} = B(\hat{\mathbf{q}})$ is a function of only coordinate variables, Eq. (A12) is simplified to the coordinate state representation as follows:

$$\hat{B} = \int d\mathbf{q}B(\mathbf{q})|\mathbf{q}\rangle\langle\mathbf{q}|. \quad \text{(A13)}$$

Similarly, one sees that Eq. (A12) becomes the momentum state representation when the operator $\hat{B} = B(\hat{\mathbf{p}})$ is a function of only momentum variables.

When the Husimi function is employed, Eq. (A2) for the operator $\hat{B}$ leads to

$$B_H(\mathbf{p},\mathbf{q}) = \left(\frac{\hbar}{2\pi}\right)^N\int d\boldsymbol{\zeta}d\boldsymbol{\eta}\exp\left(-\frac{\boldsymbol{\zeta}^T\boldsymbol{\Gamma}^{-1}\boldsymbol{\zeta}}{4} - \frac{\hbar^2}{4}\boldsymbol{\eta}^T\boldsymbol{\Gamma}\boldsymbol{\eta}\right) \times \mathrm{Tr}\left[e^{i\boldsymbol{\zeta}^T(\hat{\mathbf{q}}-\mathbf{q})+i\boldsymbol{\eta}^T(\hat{\mathbf{p}}-\mathbf{p})}\hat{B}\right] = \langle g(\mathbf{p},\mathbf{q})|\hat{B}|g(\mathbf{p},\mathbf{q})\rangle, \quad \text{(A14)}$$

and Eq. (A3) produces the dual function

$$\tilde{B}_H(\mathbf{p},\mathbf{q}) = \left(\frac{\hbar}{2\pi}\right)^N\int d\boldsymbol{\zeta}d\boldsymbol{\eta}\exp\left(\frac{\boldsymbol{\zeta}^T\boldsymbol{\Gamma}^{-1}\boldsymbol{\zeta}}{4} + \frac{\hbar^2}{4}\boldsymbol{\eta}^T\boldsymbol{\Gamma}\boldsymbol{\eta}\right) \times \mathrm{Tr}\left[e^{i\boldsymbol{\zeta}^T(\hat{\mathbf{q}}-\mathbf{q})+i\boldsymbol{\eta}^T(\hat{\mathbf{p}}-\mathbf{p})}\hat{B}\right]. \quad \text{(A15)}$$

Noting the equivalence between $\boldsymbol{\zeta}$ and $i\frac{d}{d\mathbf{q}}$ outside of the trace in the integral of Eq. (A15) and that between $\boldsymbol{\eta}$ and $i\frac{d}{d\mathbf{p}}$, we find an equivalent expression to Eq. (A15) as follows:

$$\tilde{B}_H(\mathbf{p},\mathbf{q}) = \left(\frac{\hbar}{2\pi}\right)^N\exp\left[-\frac{1}{4}\left(\frac{d}{d\mathbf{q}}\right)^T\boldsymbol{\Gamma}^{-1}\frac{d}{d\mathbf{q}} - \frac{\hbar^2}{4}\left(\frac{d}{d\mathbf{p}}\right)^T \times \boldsymbol{\Gamma}\frac{d}{d\mathbf{p}}\right]\int d\boldsymbol{\zeta}d\boldsymbol{\eta}\,\mathrm{Tr}\left[e^{i\boldsymbol{\zeta}^T(\hat{\mathbf{q}}-\mathbf{q})+i\boldsymbol{\eta}^T(\hat{\mathbf{p}}-\mathbf{p})}\hat{B}\right], \quad \text{(A16)}$$

which states that

$$\tilde{B}_H(\mathbf{p},\mathbf{q}) = \exp\left[-\frac{1}{4}\left(\frac{d}{d\mathbf{q}}\right)^T\boldsymbol{\Gamma}^{-1}\frac{d}{d\mathbf{q}} - \frac{\hbar^2}{4}\left(\frac{d}{d\mathbf{p}}\right)^T\boldsymbol{\Gamma}\frac{d}{d\mathbf{p}}\right]B_W(\mathbf{p},\mathbf{q}). \quad \text{(A17)}$$

It is straightforward to apply the same strategy to derive from Eq. (A14)

$$B_H(\mathbf{p},\mathbf{q}) = \exp\left[\frac{1}{4}\left(\frac{d}{d\mathbf{q}}\right)^T\boldsymbol{\Gamma}^{-1}\frac{d}{d\mathbf{q}} + \frac{\hbar^2}{4}\left(\frac{d}{d\mathbf{p}}\right)^T\boldsymbol{\Gamma}\frac{d}{d\mathbf{p}}\right]B_W(\mathbf{p},\mathbf{q}). \quad \text{(A18)}$$

Equation (A18) leads to a more well-known relation between the Wigner and Husimi (distribution) functions[70,71] as follows:

$$B_W(\mathbf{p},\mathbf{q}) = \exp\left[-\frac{1}{4}\left(\frac{d}{d\mathbf{q}}\right)^T\boldsymbol{\Gamma}^{-1}\frac{d}{d\mathbf{q}} - \frac{\hbar^2}{4}\left(\frac{d}{d\mathbf{p}}\right)^T\boldsymbol{\Gamma}\frac{\mathrm{d}}{\mathrm{d}\mathbf{p}}\right]B_H(\mathbf{p},\mathbf{q}) \quad \text{(A19)}$$

or equivalently,[61]

$$B_H(\mathbf{p}',\mathbf{q}') = \left(\frac{1}{\pi\hbar}\right)^N \int d\mathbf{q}d\mathbf{p}\, \exp\Big[-(\mathbf{q}-\mathbf{q}')^T\boldsymbol{\Gamma}(\mathbf{q}-\mathbf{q}') - \frac{1}{\hbar^2}(\mathbf{p}-\mathbf{p}')^T\boldsymbol{\Gamma}^{-1}(\mathbf{p}-\mathbf{p}')\Big]B_W(\mathbf{p},\mathbf{q}). \tag{A20}$$

We then readily obtain from Eq. (A4) the Husimi phase space representation or coherent state representation of the operator $\hat{B}$, i.e.,

$$\hat{B} = \frac{1}{(2\pi\hbar)^N}\int d\mathbf{q}d\mathbf{p}\tilde{B}_H(\mathbf{p},\mathbf{q})|g(\mathbf{p},\mathbf{q})\rangle\langle g(\mathbf{p},\mathbf{q})|, \tag{A21}$$

which is essential to the exact reformulation of the thermal correlation function, Eq. (1.3) or Eq. (1.6) presented in this paper.

APPENDIX B: DERIVATION OF EQ. (3.13)

Using the thawed Gaussian expressions for the imaginary and real time propagations, the expression for the time dependent reactive flux (with $\tau = \frac{\beta}{2}$) simplifies to

$$F_R(t) = \int_0^\infty dx \int_{-\infty}^\infty \frac{dp}{2\pi\hbar}\frac{p}{M}\frac{\sqrt{(Re\Gamma_t)}}{\sqrt{\pi|(\Gamma_t^* G(\tau)+1)|^2}}\exp[2\gamma(\tau)] \times \exp\left(-\frac{\hbar^2\left(|\Gamma_t|^2 G(\tau)+Re\Gamma_t\right)\left[q_t - x(\tau) + \frac{p_t(Im\Gamma_t)G(\tau)}{\hbar\left(|\Gamma_t|^2G(\tau)+Re\Gamma_t\right)}\right]^2}{\hbar^2|(\Gamma_t^*G(\tau)+1)|^2}\right) \times \exp\left(-\frac{(Re\Gamma_t)G(\tau)p_t^2\left[G^2(\tau)|\Gamma_t|^2+2G(\tau)Re\Gamma_t+1\right]}{\hbar^2|(\Gamma_t^*G(\tau)+1)|^2\left(|\Gamma_t|^2G(\tau)+Re\Gamma_t\right)}\right), \tag{B1}$$

and it is understood that the initial conditions for p_t, q_t are $p, q^\ddagger$. This result is exact for a parabolic barrier since the thawed Gaussian propagators we are using are exact for quadratic potentials.

The reactive flux is given by the long time limit of the time dependent flux. Since we are assuming a single barrier potential, asymptotically in either direction, the motion becomes free particle motion. (This is not the case for the parabolic barrier; hence, the following is not applicable to the parabolic barrier case.) To obtain the reactive flux, we need the long time limit of trajectories initiated at the location of the barrier. This means that if the initial momentum is positive, then $q_t \to +\infty$, while if the initial momentum is negative, then $q_t \to -\infty$. Furthermore, it implies that in the long time limit, the final momentum is a positive (negative) constant, $p_+(p_-)$, for initial positive (negative) momentum whose energy is greater than the barrier height. Since in this long time limit the potential is a constant, we also know from solving the equation of motion for the width parameter and free particle motion that

$$\lim_{t\to\infty}\left(t^2 Re\Gamma_t\right) = \frac{M^2}{\hbar^2\Gamma} \tag{B2}$$

and

$$\lim_{t\to\infty}\left(tIm\Gamma_t\right) = -\frac{M}{\hbar}. \tag{B3}$$

Therefore, the expression for the reactive flux simplifies to

$$F_R = \lim_{t\to\infty}\int_0^\infty dx\int_{-\infty}^\infty \frac{dp}{2\pi\hbar}\frac{p}{M}\frac{\sqrt{(Re\Gamma_t)}}{\sqrt{\pi}} \times \exp\left[2\gamma(\tau) - \frac{(Re\Gamma_t)G(\tau)p_t^2}{\hbar^2\left(G(\tau)(Im\Gamma_t)^2+Re\Gamma_t\right)}\right] \times \exp\Bigg(-\left(G(\tau)(Im\Gamma_t)^2+Re\Gamma_t\right)\Bigg[q_t - x(\tau) + \frac{p_t(Im\Gamma_t)G(\tau)}{\hbar\left(G(\tau)(Im\Gamma_t)^2+Re\Gamma_t\right)}\Bigg]^2\Bigg). \tag{B4}$$

We then use the following notation for the coordinate in the long time limit:

$$q_t = \frac{p_+}{M}t\theta(p) + \frac{p_-}{M}t\theta(-p), \tag{B5}$$

and it is understood that $p_- < 0$. Energy conservation implies that

$$\frac{p_+^2}{2M} = \frac{p_-^2}{2M} + \Delta V = \frac{p^2}{2M} + V^\ddagger + \Delta V. \tag{B6}$$

One then readily sees that

$$\lim_{t\to\infty}\frac{p_t(Im\Gamma_t)G(\tau)}{\hbar\left(G(\tau)(Im\Gamma_t)^2+Re\Gamma_t\right)} = -\left[p_+\theta(p)+p_-\theta(-p)\right] \times \frac{\Gamma G(\tau)t}{M(\Gamma G(\tau)+1)}. \tag{B7}$$

Due to the fact that the potential is asymptotically constant and that the Gaussian factor in the rate expression [Eq. (B4)] forces also the variable x to be large, we find from Eq. (3.3)

$$\lim_{t\to\infty}G(\tau) = \frac{\hbar^2}{M}\tau \tag{B8}$$

and from Eq. (3.4)

$$\lim_{t\to\infty}\gamma(\tau) = 0\cdot\theta(-p) + \Delta V\tau\theta(p). \tag{B9}$$

After changing variables from x to $y = x/t$, the expression for the reactive flux simplifies considerably

$$F_R = \int_0^\infty dy\int_{-\infty}^\infty \frac{dp}{2\pi\hbar}\frac{p}{\hbar}\frac{1}{\sqrt{\pi\Gamma}}\exp\left[-\frac{p_-^2}{(\hbar^2\Gamma\tau+M)}\tau - \frac{2M(\Delta V)\theta(p)}{(\hbar^2\Gamma\tau+M)}\tau + 2(\Delta V)\theta(p)\tau\right] \times \exp\left[-\frac{M\left(\hbar^2\Gamma\tau+M\right)}{\hbar^2\Gamma}\left(\frac{[p_+\theta(p)+p_-\theta(-p)]}{(\hbar^2\Gamma\tau+M)} - y\right)^2\right]. \tag{B10}$$

The integration over y is readily carried out, and the expression for the reactive flux becomes

$$F_R = \int_{-\infty}^{\infty} \frac{dp}{4\pi\hbar} \frac{p}{\sqrt{M(\hbar^2\Gamma\tau + M)}} \times \exp\left[-\frac{p^2 + 2MV^\ddagger}{(\hbar^2\Gamma\tau + M)}\tau + 2\theta(p)\frac{(\Delta V)\hbar^2\Gamma\tau^2}{(\hbar^2\Gamma\tau + M)}\right] \times \left(1 + \left[\theta(p)\mathrm{erf}\left(p_+\sqrt{\frac{M}{\hbar^2\Gamma(\hbar^2\Gamma\tau + M)}}\right) - \theta(-p)\mathrm{erf}\left(-p_-\sqrt{\frac{M}{\hbar^2\Gamma(\hbar^2\Gamma\tau + M)}}\right)\right]\right). \quad \text{(B11)}$$

Noting the integral

$$\int_1^\infty dX\, \exp(-AX)\mathrm{erf}\left(\sqrt{BX}\right) = \frac{\sqrt{B+A}\exp(-A)\mathrm{erf}\left(\sqrt{B}\right) + \sqrt{B}\left[1 - \mathrm{erf}\left(\sqrt{B+A}\right)\right]}{A\sqrt{B+A}}, \quad \text{(B12)}$$

one finds after some tedious algebra that the reactive flux may be expressed in closed form as follows:

$$F_R = \frac{\sqrt{\hbar^2\Gamma\tau + M}}{8\pi\hbar\tau\sqrt{M}} \exp\left[-\frac{MV^\ddagger - \hbar^2\Gamma\tau(\Delta V)}{(\hbar^2\Gamma\tau + M)}2\tau\right] \times \mathrm{erf}\left(\sqrt{\frac{2M^2(V^\ddagger + \Delta V)}{\hbar^2\Gamma(\hbar^2\Gamma\tau + M)}}\right) + \frac{\sqrt{\hbar^2\Gamma\tau + M}}{8\pi\hbar\tau\sqrt{M}} \times \exp\left(-\frac{2MV^\ddagger\tau}{(\hbar^2\Gamma\tau + M)}\right) \cdot \left[\mathrm{erf}\left(\sqrt{\frac{2M^2V^\ddagger}{\hbar^2\Gamma(\hbar^2\Gamma\tau + M)}}\right) + \exp\left(2\frac{(\Delta V)\hbar^2\Gamma\tau^2}{(\hbar^2\Gamma\tau + M)}\right) - 1\right] + \frac{1}{8\pi\hbar\tau} \times \left[1 - \mathrm{erf}\left(\sqrt{\frac{2MV^\ddagger}{\hbar^2\Gamma}}\right)\right] + \frac{\exp(2(\Delta V)\tau)}{8\pi\hbar\tau} \times \left[1 - \mathrm{erf}\left(\sqrt{\frac{2M(V^\ddagger + \Delta V)}{\hbar^2\Gamma}}\right)\right], \quad \text{(B13)}$$

and this is the desired result.

APPENDIX C: DERIVATION OF EQ. (3.23)

For a parabolic barrier with barrier frequency ω, it is well known that the leading order terms in the $\hbar$ expansion for the transmission factor are

$$\kappa = 1 + \frac{\hbar^2\beta^2\omega^2}{24} + \frac{7\hbar^4\beta^4\omega^4}{360 \cdot 16} + O\left(\hbar^6\right). \quad \text{(C1)}$$

The exact energy dependent reaction probability, as derived by Eckart,[40] is

$$P(E) = \frac{\sinh^2(\pi k)}{\cosh^2(\pi\nu_I) + \sinh^2(\pi k)} = \frac{\sinh^2\left(\frac{\pi}{\alpha}\sqrt{\frac{E}{V^\ddagger}}\right)}{\cosh^2\left(\frac{\pi}{\alpha}\sqrt{1 - \frac{1}{4}\alpha^2}\right) + \sinh^2\left(\frac{\pi}{\alpha}\sqrt{\frac{E}{V^\ddagger}}\right)}. \quad \text{(C2)}$$

As noted by Yasumori[41] (see also Ref. 72), an excellent approximation to the energy dependent probability is

$$P(E) \simeq \left\{1 + \exp\left[\frac{2\pi}{\alpha}\left(\sqrt{\left(1 - \frac{\alpha^2}{4}\right)} - \sqrt{\frac{E}{V^\ddagger}}\right)\right]\right\}^{-1}. \quad \text{(C3)}$$

From this form, Yasumori derived an analytic expression for the thermal transmission probability as follows:

$$I = \beta\int_0^\infty dE\, \exp(-\beta E)\frac{1}{1 + \exp\left(\frac{2\pi}{\alpha}\sqrt{1 - \frac{\alpha^2}{4}} - \frac{2\pi}{\alpha}\sqrt{\frac{E}{V^\ddagger}}\right)} = \exp\left(-\beta V^\ddagger\left(1 - \frac{\alpha^2}{4}\right)\right)\left[1 + 2\sum_{m=1}^{\infty}\left(\frac{\beta V^\ddagger\alpha^2}{4\pi^2}\right)^m L_{2m} \times \left(\sqrt{\beta V^\ddagger\left(1 - \frac{\alpha^2}{4}\right)}\right)\sum_{p=1}^{\infty}\frac{(-1)^p}{p^{2m}}\right], \quad \text{(C4)}$$

with

$$L_{2m}(x) = -\left[\frac{d^{(2m)}}{dy^{(2m)}}\exp\left(-y^2\right)\right]_{y=x}\exp\left(x^2\right). \quad \text{(C5)}$$

It is then a matter of straightforward algebra to find that

$$I_0 = \exp\left(-\beta V^\ddagger\left(1 - \frac{\alpha^2}{4}\right)\right), \quad \text{(C6)}$$

$$I_1 = -\frac{\beta V^\ddagger\alpha^2}{12}\exp\left(-\beta V^\ddagger\left(1 - \frac{\alpha^2}{4}\right)\right)\left[1 - 2\beta V^\ddagger\left(1 - \frac{\alpha^2}{4}\right)\right], \quad \text{(C7)}$$

$$I_2 = -\frac{7\pi^4}{360}\exp\left(-\beta V^\ddagger\left(1 - \frac{\alpha^2}{4}\right)\right)\left(\frac{\beta V^\ddagger\alpha^2}{4\pi^2}\right)^2 \times \left[48\beta V^\ddagger\left(1 - \frac{\alpha^2}{4}\right) - 16\left(\beta V^\ddagger\left(1 - \frac{\alpha^2}{4}\right)\right)^2 - 12\right] \quad \text{(C8)}$$

so that

$$I_0 + I_1 + I_2 = \exp\left(-\beta V^\ddagger\right)\left[1 + \frac{\alpha^2\beta V^\ddagger}{6}\left(1 + \beta V^\ddagger\right) + \frac{\alpha^4\left(\beta V^\ddagger\right)^2}{360}\left[9 + 7\left(\beta V^\ddagger\right)^2 - 6\beta V^\ddagger\right]\right] + O\left(\alpha^6\right), \quad \text{(C9)}$$

and this is the desired result. Note that the term $\frac{\alpha^2(\beta V^\ddagger)^2}{6}$ is identical to the term of order $\hbar^2$ for the parabolic barrier [see Eq. (C1)], while the term with $7(\beta V^\ddagger)^2$ is identical to the fourth order term of the parabolic barrier.

APPENDIX D: h^2 EXPANSION FOR THE ASYMMETRIC ECKART BARRIER

For the asymmetric Eckart barrier, the exact energy dependent transmission probability is

$$T(E) = 1 - \frac{\cosh\left[\frac{3\pi}{\alpha}\left(\sqrt{\left(\frac{E}{V_1}+3\right)}-\sqrt{\frac{E}{V_1}}\right)\right]+\cosh\left[\pi\sqrt{\frac{81}{\alpha^2}-1}\right]}{\cosh\left[\frac{3\pi}{\alpha}\left(\sqrt{\left(\frac{E}{V_1}+3\right)}+\sqrt{\frac{E}{V_1}}\right)\right]+\cosh\left[\pi\sqrt{\frac{81}{\alpha^2}-1}\right]}. \tag{D1}$$

The numerically exact transmission probabilities given in Table II are obtained by numerical quadrature of the thermal average,

$$P(\beta) = \exp(\beta V_1)\beta\int_0^\infty dE\,\exp(-\beta E)T(E). \tag{D2}$$

Our objective is to obtain an expansion of the transmission probability in $\hbar^2$ up to $\hbar^4$. For this purpose, we are guided by the result for the symmetric case, as in Eq. (3.23). Introducing four parameters $\{\gamma_j, j = 1,\ldots,4\}$, we write down the expansion for the asymmetric case as

$$P(\beta) = \left[1 + \frac{\alpha^2\beta V^\ddagger}{6}\left(\frac{3}{8}\gamma_1 + \beta V^\ddagger\right) + \frac{\alpha^4(\beta V^\ddagger)^2}{360} \times\left[9\gamma_2 + 7\gamma_4(\beta V^\ddagger)^2 - 6\gamma_3\beta V^\ddagger\right]\right] + O(\alpha^6) \tag{D3}$$

and note that using the reduced variables, this may also be rewritten exactly as a series in the reduced temperature variable τ, including up to fourth order terms,

$$P(\beta) = 1 + \frac{3\tau\alpha_s}{48}\gamma_1 + \frac{\tau^2}{6} + \frac{\alpha_s^2\tau^2}{40}\gamma_2 - \frac{\alpha_s}{60}z\tau^3\gamma_3 + \gamma\frac{7\tau^4}{360}\gamma_4. \tag{D4}$$

The parameters are then determined by computing the exact thermal transmission factor at high temperature and fitting the results to a fourth order polynomial in τ. This was implemented by computing the exact transmission probability for the values $\tau = 0.01, 0.02, 0.03, 0.04, 0.05, 0.10, 0.15, 0.2, 0.25, 0.3, 0.35$, and 0.4. The resulting coefficients with standard deviations for the expansion in τ were $0.016\,267\,82 \pm 7\times10^{-8}$, $0.165\,633 \pm 1\times10^{-6}$, $-0.005\,804 \pm 4\times10^{-6}$, and $0.018\,516 \pm 6\times10^{-6}$ for the respective powers of τ, τ^2, τ^3, and τ^4. From these and Eq. (D4), the parameters $\gamma_1, \gamma_2, \gamma_3$, and γ_4 were extracted, and they are 0.994 216, −0.603 136, 1.330 056, and 0.952 238, respectively.

Using the leading order expansion of the thawed Gaussian expression as in the symmetric case and equating the terms with $\hbar^2$ and $\hbar^4$, one obtains the temperature dependence of the width parameter coefficients Γ_0 and Γ_1.

REFERENCES

[1] R. Car and M. Parrinello, Phys. Rev. Lett. **55**, 2471 (1985).
[2] N. L. Doltsinis and D. Marx, J. Theor. Comput. Chem. **01**, 319 (2002).
[3] H. B. Schlegel, Bull. Korean Chem. Soc. **24**, 837 (2003).
[4] J. P. Klinman and A. R. Offenbacher, Acc. Chem. Res. **51**, 1966–1974 (2018) and references therein.
[5] J. Cao and G. A. Voth, J. Chem. Phys. **101**, 6157 (1994).
[6] I. R. Craig and D. E. Manolopoulos, J. Chem. Phys. **121**, 3368 (2004).
[7] D. V. Shalashilin and I. Burghardt, J. Chem. Phys. **129**, 084104 (2008).
[8] B. F. E. Curchod, C. Rauer, P. Marquetand, L. González, and T. J. Martínez, J. Chem. Phys. **144**, 101102 (2016).
[9] E. J. Heller, J. Chem. Phys. **65**, 1289 (1976).
[10] J.-L. Liao and E. Pollak, J. Chem. Phys. **108**, 2733 (1998).
[11] J. Shao, J.-L. Liao, and E. Pollak, J. Chem. Phys. **108**, 9711 (1998).
[12] H. Wang, X. Sun, and W. H. Miller, J. Chem. Phys. **108**, 9726 (1998).
[13] X. Sun, H. Wang, and W. H. Miller, J. Chem. Phys. **109**, 7064 (1998).
[14] Q. Shi and E. Geva, J. Phys. Chem. A **107**, 9059 (2003).
[15] J. Liu and W. H. Miller, J. Chem. Phys. **131**, 074113 (2009).
[16] J. Liu, Int. J. Q. Chem. **115**, 657–670 (2015).
[17] M. Ceotto, S. Yang, and W. H. Miller, J. Chem. Phys. **122**, 044109 (2005).
[18] S. Yang and J. Cao, J. Chem. Phys. **122**, 094108 (2005).
[19] J. Liu, J. Chem. Phys. **140**, 224107 (2014).
[20] J. Liu and Z. Zhang, J. Chem. Phys. **144**, 034307 (2016).
[21] W. H. Miller, R. Hernandez, N. C. Handy, D. Jayatilaka, and A. Willetts, Chem. Phys. Lett. **172**, 62 (1990).
[22] R. Hernandez and W. H. Miller, Chem. Phys. Lett. **214**, 129 (1993).
[23] P. Goel and J. F. Stanton, J. Chem. Phys. **149**, 134109 (2018).
[24] X. Shan, T. A. H. Burd, and D. C. Clary, J. Phys. Chem. A **123**, 4639 (2019).
[25] J. Tatchen and E. Pollak, J. Chem. Phys. **130**, 041103 (2009).
[26] R. Ianconescu and E. Pollak, J. Chem. Phys. **134**, 234305 (2011).
[27] M. Micciarelli, F. Gabas, R. Conte, and M. Ceotto, J. Chem. Phys. **150**, 184113 (2019).
[28] M. Kryvohuz, J. Phys. Chem. A **118**, 535–544 (2014).
[29] C. Aieta, F. Gabas, and M. Ceotto, J. Chem. Theory Comput. **15**, 2142 (2019).
[30] J. Vaníček and T. Begušić, in *Molecular Spectroscopy and Quantum Dynamics*, edited by R. Marquardt and M. Quack (Elsevier, 2021), Chapter 6, pp. 199–229.
[31] W. H. Miller, S. D. Schwartz, and J. W. Tromp, J. Chem. Phys. **79**, 4889 (1983).
[32] R. Kubo, M. Toda, and N. Hashitsume, *Statistical Physics II: Nonequilibrium Statistical Mechanics* (Springer Verlag, Heidelberg, 1991).
[33] R. Zwanzig, *Nonequilibrium Statistical Mechanics* (Oxford University Press, New York, 2001).
[34] J. Liu and W. H. Miller, J. Chem. Phys. **127**, 114506 (2007).
[35] X. Liu, L. Zhang, and J. Liu, J. Chem. Phys. **154**, 184104 (2021).
[36] M. Hillery, R. F. O'Connell, M. O. Scully, and E. P. Wigner, Phys. Rep. **106**, 121 (1984).
[37] W. J. Taylor, J. Math. Phys. **19**, 52 (1978) and references therein.
[38] F. J. McLafferty and P. Pechukas, Chem. Phys. Lett. **27**, 511 (1974).
[39] M. F. Herman and E. Kluk, Chem. Phys. **91**, 27 (1984).
[40] C. Eckart, Phys. Rev. **35**, 1303 (1935).
[41] I. Yasumori and K. Fueki, J. Chem. Phys. **22**, 1790 (1954).
[42] E. Wigner, Z. Phys. Chem **19B**, 203 (1932).
[43] B. Hellsing, A. Nitzan, and H. Metiu, Chem. Phys. Lett. **123**, 523 (1986).
[44] P. A. Frantsuzov and V. A. Mandelshtam, J. Chem. Phys. **121**, 9247–9256 (2004).
[45] E. J. Heller, J. Chem. Phys. **62**, 1544 (1975).
[46] E. Pollak and B. Eckhardt, Phys. Rev. E **58**, 5436 (1998).
[47] G. A. Voth, D. Chandler, and W. H. Miller, J. Chem. Phys. **91**, 7749 (1989).
[48] J. Cao, J. Chem. Phys. **105**, 6856 (1996).
[49] I. R. Craig and D. E. Manolopoulos, J. Chem. Phys. **123**, 034102 (2005).
[50] J. O. Richardson and S. C. Althorpe, J. Chem. Phys. **131**, 214106 (2009).
[51] N. T. Maitra and E. J. Heller, Phys. Rev. Lett. **78**, 3035 (1997).
[52] D. H. Zhang and E. Pollak, Phys. Rev. Lett. **93**, 140401 (2004).

[53]M. Gandolfi, A. Rognoni, C. Aieta, R. Conte, and M. Ceotto, J. Chem. Phys. **153**, 204104 (2020).
[54]T. Begušić and J. Vaníček, J. Chem. Phys. **153**, 024105 (2020).
[55]T. Begušić and J. Vaníček, CHIMIA **75**, 261 (2021).
[56]W. H. Miller, J. Chem. Phys. **62**, 1899 (1975).
[57]E. Pollak and J. Shao, J. Phys. Chem. A **107**, 7112 (2003).
[58]J. Shao and E. Pollak, J. Chem. Phys. **125**, 133502 (2006).
[59]E. Pollak, in *Quantum Dynamics of Complex Molecular Systems*, edited by D. A. Micha and I. Burghardt (Springer, Berlin, 2007), p. 259–273.
[60]L. Cohen, J. Math. Phys. **7**, 781 (1966).
[61]H.-W. Lee, Phys. Rep. **259**, 147 (1995).
[62]J. Liu and W. H. Miller, J. Chem. Phys. **134**, 104101 (2011).
[63]J. Liu, X. He, and B. Wu, Acc. Chem. Res. **54**, 4215 (2021).
[64]X. He, B. Wu, Y. Shang, B. Li, X. Cheng, and J. Liu, Wiley Interdiscip. Rev. Comput. Mol. Sci. e1619 (published online 2022).
[65]X. He and J. Liu, J. Chem. Phys. **151**, 024105 (2019).
[66]X. He, Z. Gong, B. Wu, and J. Liu, J. Phys. Chem. Lett. **12**, 2496–2501 (2021).
[67]X. He, B. Wu, Z. Gong, and J. Liu, J. Phys. Chem. A **125**, 6845–6863 (2021).
[68]E. Wigner, Phys. Rev. **40**, 749–759 (1932).
[69]K. Husimi, Proc. Phys. Math. Soc. **22**, 264–314 (1940).
[70]A. Voros, Phys. Rev. A **40**, 6814 (1989).
[71]M. Thoss, H. Wang, and W. H. Miller, J. Chem. Phys. **114**, 9220–9235 (2001).
[72]I. Shavitt, J. Chem. Phys. **31**, 1359 (1959).